RSC Advances

PAPER

View Article Online
View Journal | View Issue

Cite this: *RSC Adv.*, 2022, **12**, 17740

Aqueous lubrication and wear properties of nonionic bottle-brush polymers†

Hwi Hyun Moon,[a] Eun Jung Choi,[a] Sang Ho Yun,[a] Youn Chul Kim,[b] Thathan Premkumar*[ac] and Changsik Song *[a]

Received 28th April 2022
Accepted 9th June 2022

DOI: 10.1039/d2ra02711a

rsc.li/rsc-advances

The usage of aqueous lubricants in eco-friendly bio-medical friction systems has attracted significant attention. Several bottle-brush polymers with generally ionic functional groups have been developed based on the structure of biological lubricant lubricin. However, hydrophilic nonionic brush polymers have attracted less attention, especially in terms of wear properties. We developed bottle-brush polymers (BP) using hydrophilic 2-hydroxyethyl methacrylate (HEMA), a highly biocompatible yet nonionic molecule. The lubrication properties of polymer films were analyzed in an aqueous state using a ball-on-disk, which revealed that BPHEMA showed a lower aqueous friction coefficient than linear poly(HEMA), even lower than hyaluronic acid (HA) and polyvinyl alcohol (PVA), which are widely used as lubricating polymers. Significantly, we discovered that the combination of HA, PVA, and BPHEMA is demonstrated to be essential in influencing the surface wear properties; the ratio of 1 : 2 (HA : BPHEMA) had the maximum wear resistance, despite a slight increase in the aqueous friction coefficient.

1. Introduction

In recent years, research achievements in the field of tribology have progressed rapidly. Research on lubrication in an aqueous medium is specifically being conducted with a high interest in biology, biomedical engineering, and manufacturing engineering.[1–3] The aqueous lubricant is a potential for eco-friendly lubricants.[4–7] Economically, water is a comparatively cheaper and richer source than oil, while it is safe and biocompatible. In terms of functionality, it can act as an excellent coolant.[8–10]

According to length and load scale, aqueous lubrication research can be classified into microscopic and macroscopic.[11,12] Macroscopic studies of lubricants examine their frictional properties using pin-on-disk or ball-on-disk, whereas microscopic studies utilize surface force apparatus or atomic force microscope according to report.[13–15] Although some studies have been reported on microscopic properties of aqueous lubrication,[16–18] there are fewer studies available that consider macroscopic properties. This is because contact pressure becomes locally much higher than the nominal value and is challenging to regulate. However, macroscopic studies are significant because lubrication properties at real-contact regions can be implemented in macro size. As a result, we focused our efforts on analyzing the macroscopic lubrication properties for bottle-brush polymers (BP) using the ball-on-disk approach (Fig. 1).

The bottle-brush structure is key to our body's lubricating properties, especially in synovial fluid.[19,20] Lubricin, which provides boundary lubrication of articular joints, consists of long, heavily glycosylated mucinous domains in a central region, and it has a bottle-brush structure with a polypeptide backbone.[21] Many studies have been done to mimic lubricin as synthetic BP with various side chain length and different charge. For example, Claesson and coworkers showed that the decreasing the number of side chains in the interfacial region resulted in an increase in the friction coefficient.[22] In addition, Kalin and coworkers presented that the more viscous or longer the molecular chain, the greater the friction and the greater the wear protection under boundary-lubrication conditions.[23] But these polymers mostly use ionic brushes, such as cation,[24,25] anion,[26,27] zwitterion.[28,29] Lubrication studies utilizing nonionic BP are relatively rare. Here, we synthesized BP using nonionic, but hydrophilic brush chains for aqueous lubrication, since nonionic polymers are known to aggregate less than charged polymers.[30–32]

Norbornene is a versatile bridged cyclic olefin that can produce various polymers including BP *via* ring-opening metathesis polymerization (ROMP).[33–35] We combined norbornene with a chain transfer agent (CTA) moiety, capable of reversible addition fragmentation chain transfer (RAFT) reaction, to synthesize a bottle-brush polymer because of its capacity to bind various functional groups. In this case, a 2-

[a]*Department of Chemistry, Sungkyunkwan University, Suwon, Gyeonggi 16419, Republic of Korea. E-mail: tprem@skku.edu; songcs@skku.edu*

[b]*Department of Chemical Engineering, Sungkyunkwan University, Suwon, Gyeonggi 16419, Republic of Korea*

[c]*The University College, Sungkyunkwan University, Suwon, Gyeonggi 16419, Republic of Korea*

† Electronic supplementary information (ESI) available. See https://doi.org/10.1039/d2ra02711a

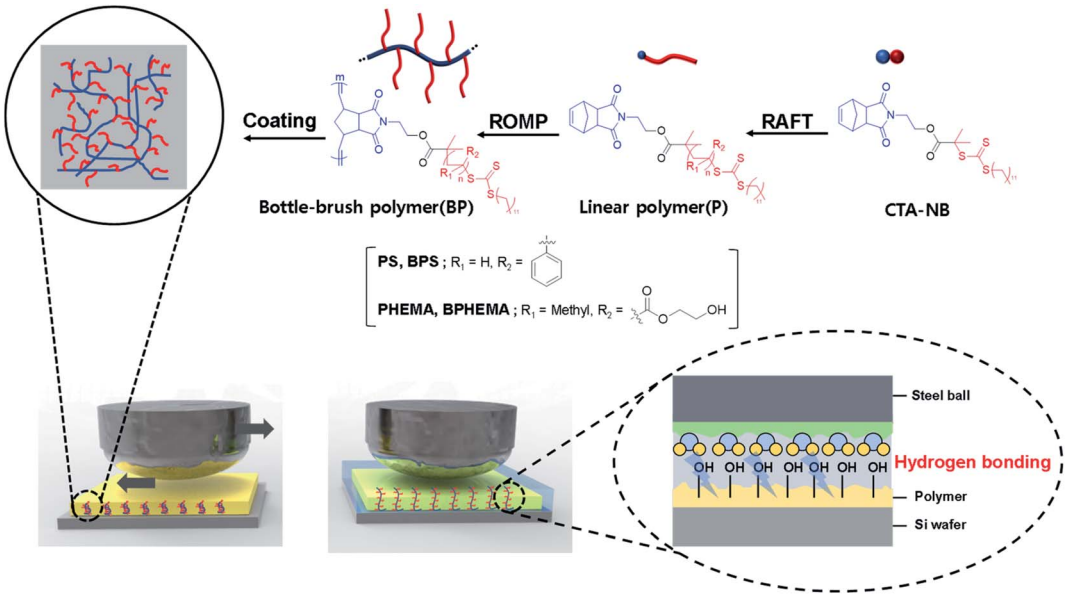

Fig. 1 The hydration lubrication properties of BP were conducted by changing the chemical composition of polymer (hydrophilic HEMA, and hydrophobic styrene) and the presence of water. Polymers demonstrated secondary interaction with steel balls resulting in high friction in the dry state.

hydroxyethyl methacrylate (HEMA) polymer was utilized as the side chain of the bottle-brush structure. HEMA is a common monomer used in soft contact lenses and has excellent blood and biocompatibility.[36–39] However, the lubricating properties of poly(HEMA) are little known, especially in the bottle-brush type structures.

When analyzing lubricated surfaces, wear properties are considered as important as a low coefficient of friction.[40,41] Continued loading can damage the surface, so any attempt to improve anti-wear will increase the lifetime of the surface. Therefore, various ways of preventing wear were proposed such as nanoparticle/fiber-reinforcements,[42,43] double network,[44,45] and interpenetrating polymer hydrogels.[46,47] The above-mentioned is a way to increase the mechanical strength by high crosslinking through the polymer composites. Accordingly, we attempted to improve abrasion characteristics by combining a bottle-brush polymer with a low coefficient of friction with natural or synthetic polymers such as hyaluronic acid (HA) and poly(vinyl alcohol) (PVA). HA is a representative substances among the moisturizing chemical in our bodies.[48,49] PVA is being researched as an artificial replacement lubricant because of its high biocompatibility and low toxicity.[50–52] We conducted a series of experiments to determine how the combining ratio of HA and PVA with synthetic polymers affects lubrication properties and wear characteristics.

2. Experimental

2.1 Materials and measurements

Alfa Aesar (MA, USA) supplied the *cis*-5-norbornene-*exo*-2,3-dicarboxylic anhydride and 2-bromoisobutyric acid. Tokyo Chemical Industry Co., Ltd (Tokyo, Japan) received 2-aminoethanol and 1-dodecanethiol. α,α'-Azobisisobutyronitrile was purchased from Junsei Chemical (Tokyo, Japan), carbon disulfide was purchased from Sigma Aldrich (MO, USA), Samchun chemicals (Seoul, Korea) received *N*,*N*′-dicyclohexyl carbodiimide and 4-dimethylaminopyridine. Proton nuclear magnetic resonance (^{1}H NMR) spectra were collected utilizing a Bruker 500 MHz spectrometer (Bruker, MA, USA). And carbon nuclear magnetic resonance (^{13}C NMR) spectra were recorded using a 125 MHz spectrometer with complete proton decoupling. The average molecular weight and polydispersity index (PDI) of the polymers were determined utilizing Agilent Technology 1260 Infinity equipment (Agilent, CA, USA) *via* gel permeation chromatography (GPC) with dimethylformamide (DMF) as the eluent and polystyrene as the standard. Fourier-transform infrared (FT-IR) spectra were recorded utilizing a spectrometer Vertex70 (Bruker Optics, MA, USA), equipped with a diamond attenuated total reflection unit. Friction coefficients were evaluated using a ball-on-disk tribometer (Anton Paar GmbH, Graz, Austria). Differential scanning calorimetry (DSC) tests were carried out on the DSC Q100 (TA Instruments, DE, USA). Rheological properties were used with rheometer MCR 302e (Anton paar, Graz, Austria).

2.2 Methods

2.2.1 Synthesis of *exo*-norbornene-imide (1). The synthesis was conducted according to the procedure identified in the study.[53] *cis*-5-norbornene-*exo*-2,3-dicarboxylic anhydride (3.0 g, 0.018 mol) was introduced to a 250 mL two-neck round bottom flask with a magnetic stir bar and dissolved in 30 mL of toluene under N_2. The flask was injected with 2-aminoethanol (2.20 g, 0.0365 mol) and triethylamine (0.550 g, 5.40 mmol) and the resulting mixture was heated to reflux for 12 h at 120 °C. After cooling to room temperature, the reaction mixture was

dissolved in CH_2Cl_2 and washed with 0.1 M HCl solution and brine. The organic layer was dried over Na_2SO_4 and the product was obtained as white powder, while the solvent was removed utilizing a rotor-evaporator. (2.80 g, 81.0% yield) ^{1}H NMR ($CDCl_3$): 1.33 (d, 1H), 1.49 (m, 1H), 2.45 (s, 1H), 2.69 (s, 2H), 3.25 (s, 2H), 3.67 (m, 2H), 3.74 (m, 2H), 6.30 (s, 1H). ^{13}C NMR ($CDCl_3$): 178.7, 137.8, 59.9, 47.9, 45.2, 42.8, 41.2.

2.2.2 Synthesis of 2-(dodecylthiocarbonothioylthio)-2-methylpropanoic acid (CTA, 2). The synthesis was conducted according to the procedure identified in the study.[54] Potassium phosphate tribasic (1.00 g, 6.60 mmol) was introduced to a 100 mL two-neck round bottom flask containing a magnetic stir bar and dissolved in 30 mL of acetone at room temperature. After 20 min of stirring, 1-dodecanethiol (1.30 g, 6.60 mmol) was introduced into the flask. Carbon disulfide (1.40 g, 18.0 mmol) was injected dropwise after an additional 20 min of stirring. The solution takes on a yellow color. After the resulting mixture was stirred for 4 h, 2-bromoisobutyric acid (1.40 g, 6.00 mmol) was introduced and stirred overnight. The organic extract was washed with water and brine after the reaction mixture was extracted with 1 M HCl and CH_2Cl_2. The organic layer was dried over $MgSO_4$ and evaporated using a vacuum. After drying, the crude product was purified using precipitation from cold hexane. (1.10 g, 78.0% yield) ^{1}H NMR ($CDCl_3$): 0.88 (3H, t), 1.38–1.26 (20H, t), 1.73 (6H, s), 3.28 (2H, t). ^{13}C NMR ($CDCl_3$): 178.6, 55.5, 37.1, 31.9, 29.6, 29.6, 29.5, 29.4, 29.3, 29.1, 28.9, 27.8, 25.2, 22.7, 14.1.

2.2.3 Synthesis of CTA-NB. The synthesis was conducted according to the procedure identified in the study.[54] *Exo*-norbornene-imide (113.5 mg, 0.545 mmol), CTA (0.200 g, 0.545 mmol), 4-dimethylaminopyridine (6.50 mg, 0.0545 mmol), and 5 mL of CH_2Cl_2 were introduced to a 25 mL round bottom flask equipped with a magnetic stir bar. The reaction mixture was stirred for 5 min, and *N*,*N*′-dicyclohexylcarbodiimide (123 mg, 0.595 mmol) was slowly introduced to the reaction flask and the resulting mixture was stirred at room temperature for 3 h. The solid was filtered and the filtrate was dry-loaded onto a silica column. The product was purified using column chromatography on silica gel with ethyl acetate/hexane (3/1, v/v) as the eluent. (38 mg, 17% yield) ^{1}H NMR ($CDCl_3$): 0.88 (3H, t), 1.40–1.26 (20H, m), 1.55 (2H, d), 1.67–1.61 (7H, m), 2.69 (2H, s), 3.28 (2H, t), 3.24 (2H, s) 3.77 (2H, t), 4.27 (2H, t), 6.29 (2H, t). ^{13}C NMR ($CDCl_3$): 177.6, 172.6, 137.8, 62.2, 55.8, 47.9, 45.2, 42.8, 37.4, 37.0, 31.9, 29.6, 29.6, 29.5, 29.4, 29.3, 29.1, 28.9, 27.8, 25.1, 22.6, 14.1.

2.2.4 Synthesis of linear polymers PS and PHEMA by RAFT. The following is a common polymer brush polymerization procedure: CTA-NB, 2,2-azobis(isobutyronitrile) (AIBN), monomer (styrene or HEMA), and solvent (100 mg mL^{-1}) were introduced to a Schlenk tube using a stir bar. The reaction mixture was deoxygenated using three freeze–pump–thaw cycles. The Schlenk tube was constant at 75 °C in N_2 atmosphere. The product is purified using precipitation from MeOH. (PS; 67 mg, 67.0%, PHEMA; 60.5 mg, 60.5%)

2.2.5 Synthesis of BPS. PS (20.0 mg) was dissolved in 0.300 mL of distilled tetrahydrofuran (THF), and Grubbs catalyst 3rd generation solution (G3) (10.0 mol%) was introduced into the solution. The solution was then stirred at room temperature for 5 h. The product is purified using precipitation from MeOH (15.0 mg, 75.0% yield).

2.2.6 Synthesis of BPHEMA. In 0.4 mL of distilled DMF, poly-CTA (20 mg) was dissolved. G3 (10 mol%) solution was introduced into the mixture, which was stirred for 5 h at room temperature. The product was precipitated from MeOH (12.0 mg, 60.0%).

2.2.7 Friction and wear test. Macroscopic friction experiments were conducted in air and water at room temperature using a conventional ball-on-disk tribometer. The friction coefficient was determined using a pin-on-disk tribometer TRB^3. Loading 1 N, we utilized a steel uncoated ball with a 6.00 mm dimension. The sliding speed was 1 cm s^{-1}. The TRB^3 sliding test was utilized to determine the depth and width of the wear track.

2.2.8 Differential scanning calorimetry (DSC) tests. Differential scanning calorimetry in N_2 condition. The sample was prepared as a powder form. Measure the glass transition temperature (T_g) as a function of temperature from −40 °C to 200 °C at 10 °C min^{-1} heating rate.

2.2.9 Rheometer tests

Rheological properties were used with rheometer MCR 302e with 8 mm parallel plates at 0.1–100 rad s^{-1} frequency range. The storage modulus (G') and loss modulus (G'') were measured for linear viscoelastic curve with time–temperature superposition at T_g + 40 °C.

3. Results and discussion

3.1 Synthesis and characterization of BP

The bottle-brush polymer BPHEMA was designed by mimicking the structure of lubricating protein lubricin, in human cartilage. The BPHEMA structure may be advantageous to contain a larger volume of water molecules due to its side chain when compared to its linear structure. We used the RAFT and ROMP reactions to synthesize the BPHEMA.

The BPHEMA was synthesized using monomers of hydrophilic HEMA and hydrophobic styrene (Scheme 1) by combining the RAFT and ROMP process. For comparison, the bottle-brush polystyrene (BPS) was also prepared. In other words, monomers of styrene and HEMA were used in preparing the linear polymers (PS and PHEMA) using the RAFT polymerization reaction. Furthermore, the BPHEMA structure was achieved using ROMP reaction as demonstrated in Scheme 1. The formation of the BPHEMA was verified using GPC analysis, which demonstrates increasing molecular weight after ROMP reactions. For example, the molecular weight of linear polymer (P) of HEMA and styrene is 6.8 k and 2.3 k (Table S1†), respectively. Under 10 k molecular weight could be reacted well with ROMP.[54] According to the GPC analysis (Fig. S1†), the polymers' molecular weight distribution changes to higher molecular weight after the ROMP reaction. The molecular weight of the BPHEMA generated by the ROMP process is 49.3 k, whereas the molecular weight of BPS is 14 k after ROMP reaction of the corresponding

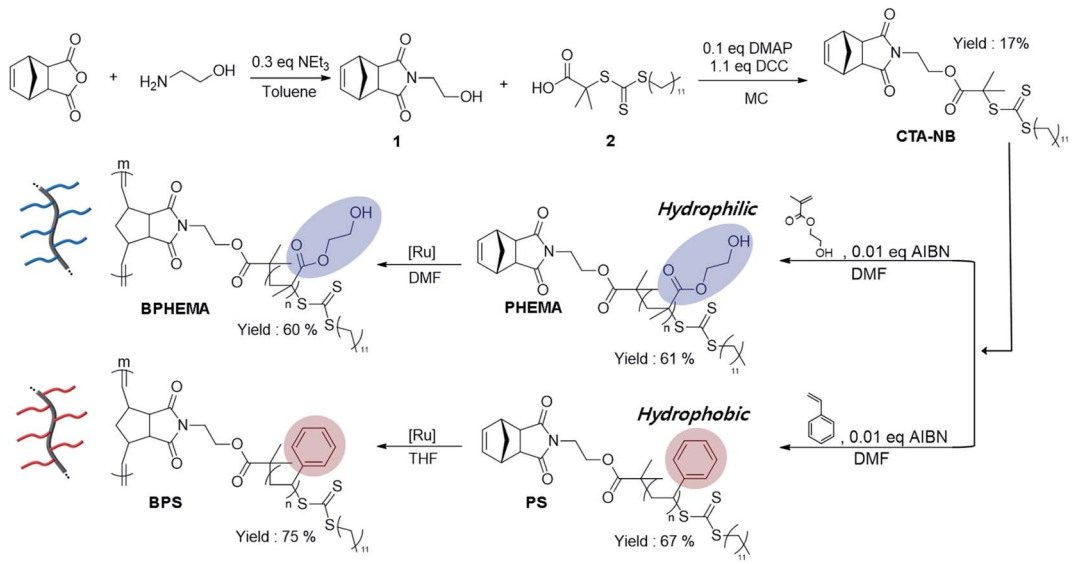

Scheme 1 Synthetic route of the bottle-brush polymer HEMA (BPHEMA) and bottle-brush polymer styrene (BPS).

linear polymer (PS). With synthesized polymers, we can also confirm that each polymer's T_g with DSC (Table S4†), and storage modulus master curve for difference of linear and bottle-brush structure (Fig. S3†). From the G' master curve of PS, and BPS, it was assumed that they have entanglement of the side chains as there is a plateau region in the case of the bottle-brush polymer.[55] Further, it was observed that the plateau region was obtained in the low-frequency portion in the case of the bottle-brush polymer, which corroborates the backbone relaxation effect.

3.2 Lubrication properties of polymers

To determine the lubrication properties of as-synthesized linear P and bottle-brush BP, the ball-on-disk experiment was conducted in water. The as-synthesized polymer was coated on Si-wafer using spin-coating. To analyze the lubrication action of a single layer of polymer, polymers were coated thinly. An ellipsometer was used to determine the thickness of PHEMA, BPHEMA, and BPS, which were 25 nm, 29 nm, and 104 nm, respectively. The polymer coated Si-wafer was installed on a ball-on-disk (Fig. 2a) and the friction coefficient was evaluated under a 1 N load in dry and wet. It is expected that the lubrication properties of PHEMA and BPHEMA in wet condition would be increased (i.c, lowering friction coefficient) due to the hydrophilic nature of the polymers. As the bottle-brush structure demonstrates the ability to bind water molecules in several ways (Fig. 2b), the presence of hydrophilic region in the polymer may increase the lubrication properties.

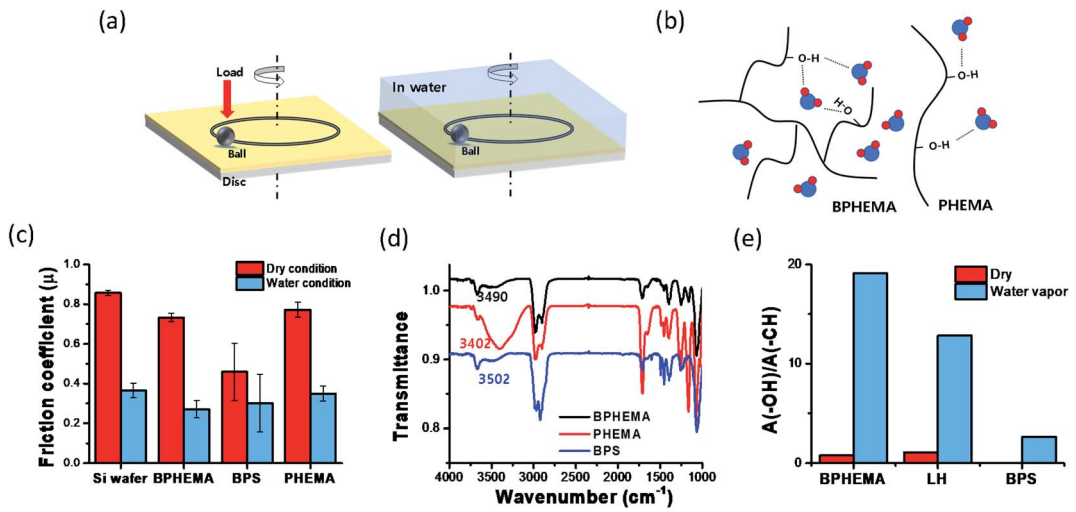

Fig. 2 (a) The schematic diagram of a ball-on-disc experiment in dry and wet. (b) The schematic model demonstrates potential hydrogen bonding formation in the BPHEMA and PHEMA structures. (c) The graph demonstrates the friction coefficient that each polymer coated on Si-wafer. (d) FT-IR spectra of BPHEMA, PHEMA, and BPS after exposure to water vapor for 12 h. (e) Graph demonstrating the ratio of FT-IR spectra hydrogen bonding strength of polymers with CH_3 bending strength.

In Fig. 2c, the friction coefficient is described by several surfaces coated with each polymer. The value of friction coefficient is specified in Table S2.† The BPS have a lower friction coefficient than BPHEMA polymers in dry state. The cause may be that the upper ball has a layer of Fe_2O_3 and partially FeOOH.[56] In the case of HEMA, the lubricating effect was low due to the influence of hydrogen bonding between the (–OH) group of the polymer and the FeOOH surfaces.

However, in water, BPHEMA demonstrates sufficients lower friction coefficient than BPS and linear PHEMA. This finding can be discussed based on the structures of polymers. BPHEMA has a comb-like structure, which water molecules can penetrate easily. There was a minimal aggregation due to the penetration of water molecules in the side chains, which allows BPHEMA a lower friction coefficient than linear polymers. In Fig. 2b, BPHEMA has the highest decreasing ratio compared to the other polymers layer.

3.3 Characterization of polymers in wet state through hydrogen bonding

The extent and strength of hydrogen bonding between polymers and water molecules has been determined. We tried to minimize hydrogen bonding interactions between water molecules using water vapor. The hydrogen bonding strength between water molecules and polymers was determined by comparing a sample exposed to water vapor for 12 h to a sample dried overnight in vacuum.

The FT-IR approach (Fig. 2d) was used to determine the quantity of hydrogen bonding between polymers and water molecules, and this allowed us to determine the influence of hydrogen bonding on lubricating properties. As shown in Fig. 2e, we can specifically determine the quantity of hydrogen bonding per CH_2 chain using two factors such as (–OH) peak shift and ratio of (–OH) peak in ~3500 cm^{-1}/(–CH) peak in ~3000 cm^{-1}.

The higher the hydrogen bonding strength between polymers and water molecules, the thicker the water lubricating layer, which increases the lubrication effect. When the peak has a higher blue shift, the strength of the hydrogen bonding between polymer and water molecules is stronger. Fig. 2d demonstrates the FT-IR spectra, its observed that the –OH peak of BPHEMA, 3490 cm^{-1}, is more blue-shifted than the –OH peak of PHEMA, 3402 cm^{-1}, which indicates the formation of stronger hydrogen bonding between BPHEMA and water than between PHEMA and water molecules. The cause can be discussed by considering the structures of the polymers. Structurally, BPHEMA can hold more water molecules (more water molecules can enter between bottle-brushes), due to its comb-like structure than the PHEMA polymer, which has a simple linear structure.[57,58] In the case of BPS, –OH peak (~3502 cm^{-1}) strength is too low because it has no functional groups capable of forming hydrogen bonding with water molecules, and only van der Waals forces acted.

The second factor is the peak ratio of A(–OH)/A(–CH), where A(–OH) represent the intensity of –OH peak (hydrogen bonding, ~3500 cm^{-1}) and A(–CH) indicates the intensity of CH_2, CH_3 bending peaks (~2900 cm^{-1}). A higher A(–OH)/A(–CH) suggests stronger hydrogen bonding formation and *vice versa*. Fig. 2e demonstrates the ratio of A(–OH)/A(–CH) in dry, in wet conditions. From this ratio, it is possible to determine the increase or decrease of hydrogen bonds with water per unit carbon.[59]

When the FT-IR spectra of PHEMA and BPHEMA are compared, the A(–OH)/A(–CH) ratio of BPHEMA as volume of CH_2 groups is higher than the PHEMA.[60] In the case of BPS, since there are no functional groups capable of forming hydrogen bonding, the ratio of A(–OH)/A(–CH) is very low. It is proven that BPHEMA has the highest A(–OH)/A(–CH) intensity ratio. As this result, it is verified that more hydrogen bonds are generated in the bottle-brush structure which demonstrates effective hydrated lubrication.

3.4 Improving wear property by combining HA and PVA with synthesized polymers

It is important that the lubricated surface is slippery, but it is also important that it withstands wear. We can observe that BPHEMA in water state have lowest friction coefficient, which signifies highest lubricating surface. We also investigated the wear characteristics of each surface. As shown in Fig. 3a, we expected improved wear properties by combining HA and PVA with the bottle-brush BPHEMA, since the polymer itself suffered from significant wear (see below).

In Fig. 3b and c, demonstrate friction coefficient graphs for the complex surface of BPHEMA with HA and PVA, respectively. The value of friction coefficient of BPHEMA complex with HA and PVA is specified in Table S3.† Overall, whether in dry or wet state, the friction coefficient of the combinations seems to be the average of each component. Therefore, combining BPHEMA

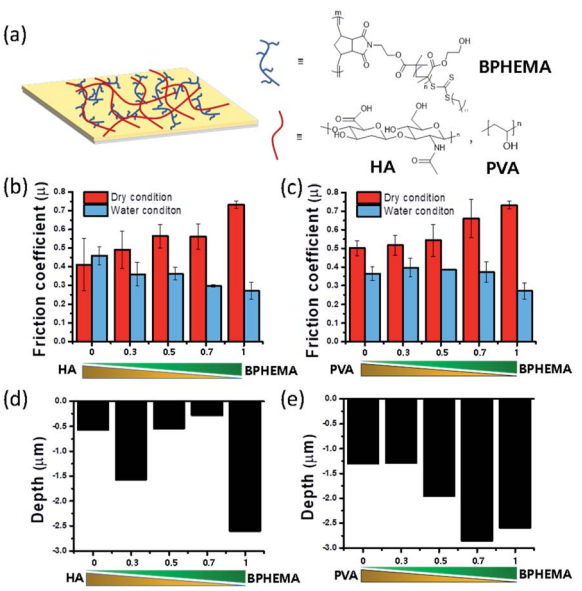

Fig. 3 (a) Scheme of BPHEMA complex with HA and PVA. The graph demonstrates the friction coefficient of complex BPHEMA with (b) HA and (c) PVA in various ratios. The depth of wear track of coated surfaces was determined by sliding test. Wear characteristics of BPHEMA combining with (d) HA and (e) PVA.

with other polymers may reduce its lubricating properties slightly.

The sliding test was utilized to evaluate the wear characteristics of the as-synthesized polymers coating by analyzing by depth and width of the wear track. During the sliding test, the surfaces are profield with various depths. In Fig. 3d and e, the wear characteristics may be analyzed by evaluating the surface depth when a load has damaged the surfaces during the sliding test. In general, all surfaces evaluated in water demonstrated less wear than in dry conditions. Specifically, HA and PVA demonstrated significant less wear than BPHEMA. HA and PVA, in particular, generate water-retaining gels when exposed to water. This is due to its excellent influence to prevent surface wear. Therefore, to get a surface with enhanced wear characteristics, HA and PVA were combined with BPHEMA at various ratios, and the coating was analyzed. It is considered that the HA and BPHEMA combination has better wear influence than only BPHEMA surface. In particular, it was confirmed that the best wear resistance could be obtained when the ratio of HA : BPHEMA (1 : 2) has the lowest wear depth (Fig. S2†). However, when PVA was combined, the synergy was not good as compared to HA, but it was confirmed that the abrasion resistance was enhanced when PVA : BPHEMA (2 : 1) which demonstrates a lower wear depth than the BPHEMA surface.

4. Conclusions

The synthesis of bottle-brush BPHEMA was conducted and the aqueous lubrication characteristics were analyzed. A norbornene-based polymer was synthesized utilizing RAFT reaction with HEMA as a hydrophilic functional group, and BPHEMA were synthesized using ROMP process. The ball-on-disc test was used to analyze the friction coefficient and determine the lubricating properties of the as-synthesized BPHEMA. The friction coefficient in water study indicated that the more hydrophilic polymers have a low friction coefficient because of the water lubricating layer exists thicker at hydrophilic surfaces. In aqueous conditions, the BPHEMA structure demonstrates a potential lubrication influence than linear polymer because the water molecules can easily penetrate the bottle-brush and generate a strong hydrogen bonding network. Furthermore, we analyzed the change of the lubrication properties depending on the combination of BPHEMA and the various ratios of common lubricants such as HA and PVA. It was observed that the ratio of BPHEMA decreased in wet condition, the friction coefficient was increased. However, it was verified that the surface could be controlled with better abrasion resistance by combining BPHEMA with HA, and PVA. In short, we identified the lubricating benefits of BPHEMA polymers and analyzed their potential to effectively demonstrate wear properties. It has potential to contribute as a material in the field of aqueous lubrication. Therefore, these findings specify the competence to generated BPHEMA using RAFT and ROMP reactions and explore its novel lubrication properties making this system a novel platform for industrial applications.

Author contributions

H. H. Moon: conceptualization, investigation, methodology, formal analysis, writing-original draft; E. J. Choi: investigation, writing-original draft; S. H. Yun: writing-review & editing; Y. C. Kim: review & editing; T. Premkumar: conceptualization, writing-review & editing; C. Song: conceptualization, investigation, writing-review & editing, supervision.

Conflicts of interest

There are no conflicts to declare.

Acknowledgements

This work was supported by the Materials and Components Technology Development Program of MOTIE/KEIT (Project No. 20013223). Also, this work was supported by the Basic Science Research Programs through the National Research Foundation (NRF) of Korea funded by the Ministry of Education (NRF-2019K1A3A1A18116050).

References

1 G. E. Yakubov, L. Macakova, S. Wilson, J. H. C. Windust and J. R. Stokes, *Tribol. Int.*, 2015, **89**, 34–45.
2 Q. B. Wei, X. W. Pei, J. Y. Hao, M. R. Cai, F. Zhou and W. M. Liu, *Adv. Mater. Interfaces*, 2014, **1**, 1400035.
3 K. Chawla, S. Lee, B. P. Lee, J. L. Dalsin, P. B. Messersmith and N. D. Spencer, *J. Biomed. Mater. Res., Part A*, 2009, **90A**, 742–749.
4 L. Zhang, Y. Guo, H. Xu, G. Li, F. Zhao and G. Zhang, *Chem. Eng. J.*, 2021, **420**, 129891.
5 L. R. Ma, C. H. Zhang and S. H. Liu, *Chin. Sci. Bull.*, 2012, **57**, 2062–2069.
6 W. H. Briscoe, *Curr. Opin. Colloid Interface Sci.*, 2017, **27**, 1–8.
7 D. Kumar, A. Singh and D. K. Mishra, *Proc. Inst. Mech. Eng., Part J*, 2016, **230**, 968–973.
8 Z. Li, S. Ma, G. Zhang, D. Wang and F. Zhou, *ACS Appl. Mater. Interfaces*, 2018, **10**, 9178–9187.
9 R. D. Han, J. Y. Liu and Y. F. Sun, *Ind. Lubr. Tribol.*, 2005, **57**, 187–192.
10 X. Deng, H. Gates, B. Weaver, H. Wood and R. Fittro, *Asme Turbo Expo*, 2018, **7B**, 75597.
11 X. Z. Huang, J. Wu, Y. D. Zhu, Y. M. Zhang, X. Feng and X. H. Lu, *Chin. J. Chem. Eng.*, 2017, **25**, 1552–1562.
12 A. Arcifa, A. Rossi, S. N. Ramakrishna, R. Espinosa-Marzal, A. Sheehan and N. D. Spencer, *J. Phys. Chem. C*, 2018, **122**, 7331–7343.
13 J. F. Li, F. Zhou and X. L. Wang, *Meccanica*, 2011, **46**, 499–507.
14 L. Hao, Z. Wang, G. Y. Zhang, Y. Y. Zhao, Q. J. Duan, Z. N. Wang, Y. Q. Chen and T. J. Li, *Mech. Ind.*, 2020, **21**, 108–114.
15 A. S. Kumar, S. Deb and S. Paul, *J. Manuf. Process.*, 2020, **56**, 766–776.

16 R. G. Wang, M. Kido, T. Tokuda, K. Kato and S. Nakanishi, *J. Jpn. Inst. Metals*, 2003, **67**, 404–409.
17 J. Q. Ren, J. S. Zhao, Z. G. Dong and P. K. Liu, *Appl. Surf. Sci.*, 2015, **346**, 84–98.
18 C. D. Lorenz, M. Chandross and G. S. Grest, *J. Adhes. Sci. Technol.*, 2010, **24**, 2453–2469.
19 Y. Q. Xia, V. Adibnia, R. L. Huang, F. Murschel, J. Faivre, G. J. Xie, M. Olszewski, G. De Crescenzo, W. Qi, Z. M. He, R. X. Su, K. Matyjaszewski and X. Banquy, *Angew. Chem., Int. Ed.*, 2019, **58**, 1308–1314.
20 X. Banquy, J. Burdynska, D. W. Lee, K. Matyjaszewski and J. Israelachvili, *J. Am. Chem. Soc.*, 2014, **136**, 6199–6202.
21 B. Zappone, G. W. Greene, E. Oroudjev, G. D. Jay and J. N. Israelachvili, *Langmuir*, 2008, **24**, 1495–1508.
22 T. Pettersson, A. Naderi, R. Makuska and P. M. Claesson, *Langmuir*, 2008, **24**, 3336–3347.
23 I. Velkavrh and M. Kalin, *Tribol. Int.*, 2012, **50**, 57–65.
24 K. Lienkamp and G. N. Tew, *Chem.–Eur. J.*, 2009, **15**, 11784–11800.
25 R. J. Dalal, R. Kumar, M. Ohnsorg, M. Brown and T. M. Reineke, *ACS Macro Lett.*, 2021, **10**, 886–893.
26 F. Zhou and W. T. S. Huck, *Chem. Commun.*, 2005, **48**, 5999–6001.
27 Z. F. Yang, V. V. Tarabara and M. L. Bruening, *Langmuir*, 2015, **31**, 11790–11799.
28 S. Samanta and J. Locklin, *Langmuir*, 2008, **24**, 9558–9565.
29 X. Xu, M. Billing, M. Ruths, H. A. Klok and J. Yu, *Chem.–Asian J.*, 2018, **13**, 3411–3436.
30 J. M. Sarapas, T. B. Martin, A. Chremos, J. F. Douglas and K. L. Beers, *Proc. Natl. Acad. Sci. U. S. A.*, 2020, **117**, 5168–5175.
31 C. R. Lopez-Barron and M. E. Shivokhin, *Phys. Rev. Lett.*, 2019, **122**, 037801.
32 S. S. Sheiko, B. S. Sumerlin and K. Matyjaszewski, *Prog. Polym. Sci.*, 2008, **33**, 759–785.
33 A. Hafner, P. A. vanderSchaaf and A. Muhlebach, *Chimia*, 1996, **50**, 131–134.
34 S. I. Subnaik and C. E. Hobbs, *Polym. Chem.*, 2019, **10**, 4524–4528.
35 D. A. N'Guyen, F. Leroux, V. Montembault, S. Pascual and L. Fontaine, *Polym. Chem.*, 2016, **7**, 1730–1738.
36 J. V. M. Weaver, I. Bannister, K. L. Robinson, X. Bories-Azeau, S. P. Armes, M. Smallridge and P. McKenna, *Macromolecules*, 2004, **37**, 2395–2403.
37 M. N. Moghadam and D. P. Pioletti, *J. Biomed. Mater. Res., Part B*, 2016, **104**, 1161–1169.
38 J.-P. Montheard, M. Chatzopoulos and D. Chappard, *J. Macromol. Sci., Polym. Rev.*, 1992, **32**, 1–34.
39 F. Fornasiero, F. Krull, C. J. Radke and J. M. Prausnitz, *Fluid Phase Equilib.*, 2005, **228**, 269–273.
40 X. G. Hu, *Polym.-Plast. Technol. Mater.*, 2000, **39**, 137–150.
41 Z. X. Li, S. H. Ma, G. Zhang, D. A. Wang and F. Zhou, *ACS Appl. Mater. Interfaces*, 2018, **10**, 9178–9187.
42 I. C. Liao, F. T. Moutos, B. T. Estes, X. H. Zhao and F. Guilak, *Adv. Funct. Mater.*, 2013, **23**, 5833–5839.
43 Y. J. No, S. Tarafder, B. Reischl, Y. Ramaswamy, C. R. Dunstan, O. Friedrich, C. H. Lee and H. Zreiqat, *ACS Biomater. Sci. Eng.*, 2020, **6**, 1887–1898.
44 Y. M. Chen, K. Dong, Z. Q. Liu and F. Xu, *Sci. China: Technol. Sci.*, 2012, **55**, 2241–2254.
45 Z. Q. Zhang, Z. S. Ye, F. Hu, W. B. Wang, S. J. Zhang, L. Gao and H. L. Lu, *J. Appl. Polym. Sci.*, 2022, **139**, 51563–51577.
46 M. Arjmandi, M. Ramezani, A. Nand and T. Neitzert, *Wear*, 2018, **406**, 194–204.
47 M. Arjmandi and M. Ramezani, *J. Mech. Behav. Biomed. Mater.*, 2019, **95**, 196–204.
48 W. Lin, Z. Liu, N. Kampf and J. Klein, *Cells*, 2020, **9**, 1606–1620.
49 C. E. T. Reinoso, C. E. G. Sinchiguano, C. A. Q. Pulupa and M. L. V. Piedra, *Rev. Cuba. Reumatol.*, 2020, **22**, 171.
50 T. Murakami, S. Yarimitsu, K. Nakashima, N. Sakai, T. Yamaguchi, Y. Sawae and A. Suzuki, *Proc. Inst. Mech. Eng., Part H*, 2015, **229**, 864–878.
51 L. C. Duque-Ossa, G. Ruiz-Pulido and D. I. Medina, *Polymers*, 2021, **13**, 746–761.
52 T. Elakkiya, R. Sheeja, K. Ramadhar and T. S. Natarajan, *J. Appl. Polym. Sci.*, 2013, **128**, 2840–2846.
53 Y. Qiao, J. Ping, H. Tian, Q. Zhang, S. Zhou, Z. Shen, S. Zheng and X. Fan, *J. Polym. Sci., Part A: Polym. Chem.*, 2015, **53**, 2116–2123.
54 S. C. Radzinski, J. C. Foster, R. C. Chapleski Jr, D. Troya and J. B. Matson, *J. Am. Chem. Soc.*, 2016, **138**, 6998–7004.
55 S. J. Dalsin, M. A. Hillmyer and F. S. Bates, *Macromolecules*, 2015, **48**, 4680–4691.
56 Y. Long, M. B. Bouchet, T. Lubrecht, T. Onodera and J. M. Martin, *Sci. Rep.*, 2019, **9**, 6286.
57 M. G. Wessels and A. Jayaraman, *Soft Matter*, 2019, **15**, 3987–3998.
58 A. Chremos, F. Horkay and J. F. Douglas, *J. Chem. Phys.*, 2021, **155**, 134905–134914.
59 O. Y. Zolotarskaya, Q. Yuan, K. J. Wynne and H. Yang, *Macromolecules*, 2013, **46**, 63–71.
60 L. Mu, Y. Shi, J. Hua, W. Zhuang and J. Zhu, *J. Phys. Chem. B*, 2017, **121**, 5669–5678.